Dynamic Responses in Nanocomposite Hydrogels

Elena Loizou,[†] Paul Butler,[‡] Lionel Porcar,[‡] and Gudrun Schmidt*,[†]

Department of Chemistry, Louisiana State University, Baton Rouge, Louisiana 70803, and
National Institute of Standards and Technology, Gaithersburg, Maryland 20899

ABSTRACT: The shear response of a series of polymer−clay gels has been investigated by means of rheology and small-angle neutron scattering (SANS). The gels have the same composition by mass but different polymer molecular weights (M_w). While long polymer chains can interconnect several platelets, which act as multifunctional cross-links, very short polymer chains should not be able to do so, allowing us to explore the effects of bridging on structure and dynamical responses. Increasing the polymer M_w in the gels leads to increasingly strong anisotropy in the SANS data, indicating a larger and larger degree of shear orientation. This relative increase in orientation, however, is accompanied by a relatively lower amount of shear thinning. Simple solutions of anisotropic particles usually shear thin by alignment of the particles with the flow, allowing them for example to slide past each other more easily. In a connected gel, breaking of the connectivity should also lead to shear thinning. Thus, the inverse relationship between shear orientation and shear thinning, combined with the fact that the lowest M_w, which exhibits the highest shear thinning, does not orient at all, supports our earlier hypothesis that the alignment mechanism in these systems stems from the coupling between the clay and the polymer mediated by the shear flow and nicely demonstrates the effect of bridging on the strength and dynamics of these gels.

Introduction

A wealth of novel materials with fascinating structures and morphologies have been discovered and engineered at the nanoscale.[1] Among these, nanocomposite polymer−clay gels and solutions are generating tremendous interest as materials with novel mechanical,[2] electrical,[3] optical,[3,4] and thermal[2,5] properties. The ability to tailor properties to the desired application by controlling nanoscopic structure can optimize the materials performance for a variety of applications. Many important nanocomposites are attractive for applications such as personal care products, pharmaceuticals, cosmetics, optical components, thin film barrier membranes, and ceramic precursor materials.

A number of studies have tried to understand, control, and manipulate the structure of nanocomposites, their polymer−clay interactions, and their shear-induced structural changes and provide a measure of the size, shape, and interfacial polymer conformation.[6−9] Solutions, gels, and solution precursors experience considerable flow during processing and, sometimes, as part of their end use. Furthermore, many properties depend on the structural changes such as the orientation of the clay platelets within the material, a property which can be greatly affected or controlled by shear flow. Thus, it is imperative to understand the polymer−clay interactions in solutions and their responses to shear.

The goal of the present study is to probe the shear response of a series of polymer−clay gels by means of rheology and small-angle neutron scattering (SANS). A model system of Laponite clay and poly(ethylene oxide) (PEO) polymer is used to form gels that have the same composition by mass and only differ in their polymer molecular weight (M_w). PEO absorbs onto charged Laponite clay platelets, and it is believed that low molecular weight polymers inhibit aggregation of clay particles by classic steric hindrance,[10] while higher molecular weight

polymers, particularly at higher concentrations of clay, bridge between particles and lead to the formation of large clusters[10] or smart gels with novel properties.[8,11−13] Recent SANS studies describe the adsorption of PEO polymer chains onto Laponite clay platelets at low polymer and clay concentrations using contrast variation methods to separate the contributions from bulk and adsorbed polymer chains.[14,15] SANS studies made with no excess polymer confirm these results but also find that the edges of the platelets have polymer density on them that is much thicker than on the face.[7] Other research groups have used neutron diffraction to look at the local segmental, salt, and water structure around each clay platelet and to understand the mechanism of bridging flocculation.[6,16]

In previous static work on the highest molecular weight of these gels we found a fractal-like network of clay rich areas with polymer-rich water pockets.[17] In this work, we study the M_w dependence of shear-induced structures and orientation, along with the shear-dependent rheology, and observe an interesting inverse relationship between ease of orientation and degree of shear thinning.

Experimental Section

In this study aqueous gels of the synthetic hectorite type clay (Southern Clay) Laponite RD (LRD) and poly(ethylene oxide) (PEO) were used.[18] The clay particles are composed of platelets of high purity and relatively uniform size (≈30 nm in diameter and ≈1 nm thick).[17] PEO with a M_w = 100, 300, 600, and 1000 kg/mol and a polydispersity (M_w/M_n) of ≈1.5 was purchased from Polysciences Inc. All the samples have a pH value of ≈10 and a NaCl concentration of 10^{-3} mol/L. Because of dissolution of CO_2 from air, a decrease of the samples' pH is observed over time. Gels whose pH dropped below 8 were discarded to avoid sample degradation. Samples prepared in D_2O seemed to be more stable at pH 10 than samples prepared in H_2O due to isotope effects, and D_2O was thus used for both the rheology and SANS experiments. Highly reproducible measurements were possible within a window of 3 months after sample preparation. The results reported here were obtained from gels containing mass fractions of 3% LRD and 2% PEO at room temperature (abbreviated as LRD3-PEO2-M_w (in kg/mol), Table 1). At equilibrium, the clay surfaces are covered

[†] Louisiana State University.
[‡] National Institute of Standards and Technology.
* Corresponding author. E-mail: gudrun@lsu.edu.

Table 1. Composition of Hydrogels[a]

name of sample	mass fraction LRD (%)	mass fraction PEO (%)	M_w of PEO (kg/mol)
LRD3-PEO2-M_w 100	3	2	100
LRD3-PEO2-M_w 300	3	2	300
LRD3-PEO2-M_w 600	3	2	600
LRD3-PEO2-M_w 1000	3	2	1000

[a] All polymer−clay gels contain 95% of D_2O by mass.

by adsorbed PEO segments[7] with any excess polymer serving as a matrix in which the clay particles diffuse, with sufficiently long polymer chains being able to "bridge" neighboring clay particles.[17] The resulting systems are macroscopically homogeneous and transparent hydrogels with near perfect clay exfoliation as evidenced by a lack of peaks at high q in SANS.[8] Extensive mixing and shear (for ≈3 weeks) was used to guarantee complete dissolution of polymer and Laponite clusters and reproducibility of rheological experiments.

Rheological experiments were performed on a Rheometrics Scientific ARES rheometer with parallel plate geometry (38 mm diameter, 1 mm gap). The shear rate dependence of the viscosity was obtained by performing individual, time-dependent, constant-rate experiments. Once the samples equilibrated to a steady-state viscosity, the viscosity was recorded, and another time-dependent, constant-rate experiment was performed. Constant shear rates were thus applied for times ranging from ≈5000 s at the lowest shear rates down to ≈20 s at the highest shear rates. To prevent solvent evaporation, a small amount of low-viscosity silicon oil was floated on top of the sample. The effect of the silicon oil on the overall rheological behavior is negligible. Duplicate measurements with a new sample showed reproducibility of steady-state values within a relative uncertainty of ≈9%.

SANS measurements were performed on the NG7 instrument[19] at the Center for Neutron Research of the National Institute of Standards and Technology. The q range used ($q = 4\pi/\lambda \sin(\theta)/2$) covered 2.27×10^{-3} Å^{-1} < q < 0.24 Å^{-1}. The shear cell is a Couette-type geometry[20] that has an inner diameter of 60 mm and a gap of 1 mm, giving a total path length of 2 mm through the sample. In the standard configuration, referred to as the "radial beam" geometry, the incident beam is parallel to the shear gradient. This geometry provides information in the flow (x)−vorticity (z) plane. Small-angle scattering investigations are excellent tools in providing quantitative information concerning structures on the 1 to ≈300 nm length scales and can detect the orientation of the clay platelets and polymer chains under shear.

Results and Discussion

Previous results from the LRD3-PEO2-M_w 1000 polymer clay gel have led to the postulate that the polymer chains are in a dynamic adsorption/desorption equilibrium with the clay particles to form a network.[8] In this network the clay platelets, covered by a 1.5 nm thick polymer coating, are dynamically tethered together in loose bundles that form fractal-like structures with "pores" up into the micrometer regime.[17] This skeleton-like structure on the nanometer and micrometer length scale would account for the lack of flow in a gel containing mass fractions of 95% of water and only 5% of dissolved solids.

In the current study, all the gels have the same mass composition, i.e., 3% LRD clay and 2% PEO (Table 1). Thus, every solution has the same total clay surface area and the same number of EO segments, the only difference being that in some gels there are many shorter PEO chains while in others there are fewer, but longer, PEO chains. The amount of PEO absorption has been suggested to be slightly molecular weight dependent; however, for the molecular weights used in this study, the reported absorption[7] is constant within errors at 0.70 ± 0.05 mg/m^2. The available specific surface area reported by the supplier is 370 m^2/g determined by the Brunauer−Emmett−
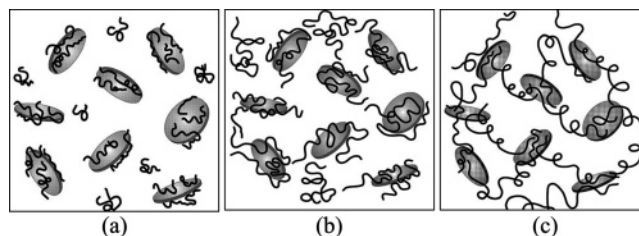

Figure 1. Schematic representation of the local structure in Laponite−PEO gels in the absence of shear, for different molecular weights of PEO. The coils represent the polymer chains and the disk-shaped particles are the clay platelets, which are completely covered with polymer. As the polymer chain length increases (due to increase of the M_w), the system has more polymer−clay interconnections.

Teller (BET) nitrogen adsorption method. This leads to a mass fraction of absorbed polymer of 0.78%, leaving 1.22% unabsorbed polymer which will clearly influence the network structure as well as the shear behavior. Various calculations of specific surface area based on purported size of the clay particles range from 700 to 900 m^2/g.[7,10,15] While these numbers are not based on any actual direct measurement of the surface area, and are extremely sensitive to the polydispersity and shape of the distribution (being proportional to the second moment) as well as the exact dimensions, we note that even for the highest reported value the absorbed amount would be 1.89%, still leaving 0.11% of excess polymer. Polymer−clay hydrogels without much excess polymer (3% clay and 1% PEO, M_w = 1000 kg/mol) are nonsticky, spongelike gels with pores from which water can be squeezed out easily. Rheological data from these samples are difficult to obtain due to wall slip and shear-induced phase separation.[8] The presence of excess PEO in our samples (3% clay and 2% PEO) appears to stabilize the structure under shear by thickening the gel, increasing the adhesion to glass and skin, and filling the large water pores.[17]

The average distance between clay platelets in a 3% clay gel has been reported to be ≈55 to 80 nm from a maximum in the SANS spectra.[8,21,22] These values are also supported by recent electron microscopy experiments,[17] calculations,[23] and other experimental evidence.[8,22] Depending on the model and the assumptions made for calculating interparticle distances, slightly different results are obtained. In the SANS results reported here there is no visible signature of interactions, but the average distance between clay platelets must remain the same. Thus, for our polymer clay gel at 3% Laponite and 2% PEO, the large molecular weight polymers, such as the M_w = 1000 kg/mol (having a hydrodynamic radius R_h ≈ 100 nm) and the M_w = 600 kg/mol (R_h ≈ 59 nm),[24] are extended enough to conceivably interconnect one or more clay platelets, while the smallest molecular weight polymer, M_w = 100 kg/mol (R_h ≈ 21 nm), cannot (Figure 1). Although all polymer−clay gels have the same excess polymer concentration, only those with long enough individual polymer chains to tie clay platelets together would be expected to significantly alter the dynamics of the system. Previous SANS experiments have shown that a polymer−clay solution with a polymer M_w = 1000 kg/mol exhibits shear-induced anisotropy in the scattering due to alignment of the nanoscopic particles, while under similar conditions a comparable pure clay solution or a pure polymer solution does not exhibit any such shear-induced anisotropy.[8]

To test the viscoelastic properties at low deformations, we have performed frequency-dependent oscillatory shear experiments, which are shown in Figure 2. These data were taken at 1% strain, well within a relatively broad linear viscoelastic range. The storage moduli G' are always larger than the loss
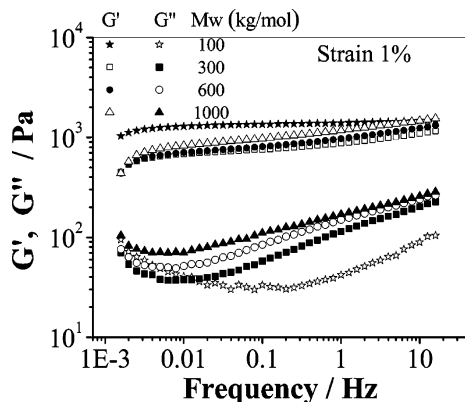
Figure 2. Frequency dependence of G' and G'' for the polymer–clay gels mentioned in Table 1. Experiments can be reproduced with a new sample within a relative standard deviation of $\approx 15\%$ for LRD3-PEO2-M_w 100 gel and smaller than 7% for the other gels.
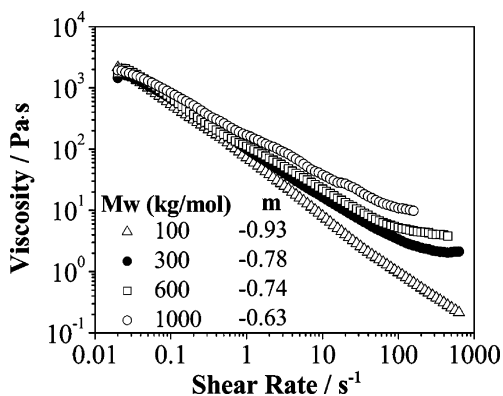
Figure 3. Steady shear viscosity (η) as a function of shear rates ($d\gamma/dt$) for the LRD3-PEO2-M_w series. Power law exponents m were obtained via $\eta = (d\gamma/dt)^m$. Experiments can be reproduced with a new sample within a relative standard deviation of $\approx 7\%$.

moduli G'', indicating the gels behave like elastic solids in this frequency range. The LRD3-PEO2-M_w 100 exhibits similar rheological characteristics to a pure 3% LRD gel, with a near-frequency-independent storage modulus.[25,26] The higher PEO molecular weight samples display some frequency-dependent storage modulus, which increases with increasing frequency and molecular weight of the sample. This may be related to the formation of a transient network in which the clay platelets are "bridged" by the PEO. At the lower frequencies, the LRD3-PEO2-M_w 100 appears to have a slightly higher elastic modulus than the other gels; however, the relative uncertainty on the moduli of the M_w 100 is $\approx 15\%$ while that of the moduli for the other gels is less than 7%.

The loss moduli, G'', all exhibit a minimum, G''_{min}, resulting from the increase in G'' at both low and high frequencies. The minimum shifts to lower frequency dramatically between the LRD3-PEO2-M_w 100 and the higher molecular weight samples while it shifts much more slowly as a function of polymer molecular weight in these higher molecular weight samples. This shift appears to be entirely due to an increase (or shift) of the high frequency mode of G'', indicating that viscous relaxation becomes increasingly dominant at the higher frequencies as the polymer molecular weight increases. At these low deformations of 1%, the flow history does not change the equilibrium structure of the gel at rest, and all experiments could be reproduced when repeated. SANS at these deformations showed no anisotropy.

The steady-state viscosities from LRD3-PEO2-M_w 100, 300, 600, 1000 gels are shown in Figure 3. All the gels shear thin over the entire range of shear rates and give power law
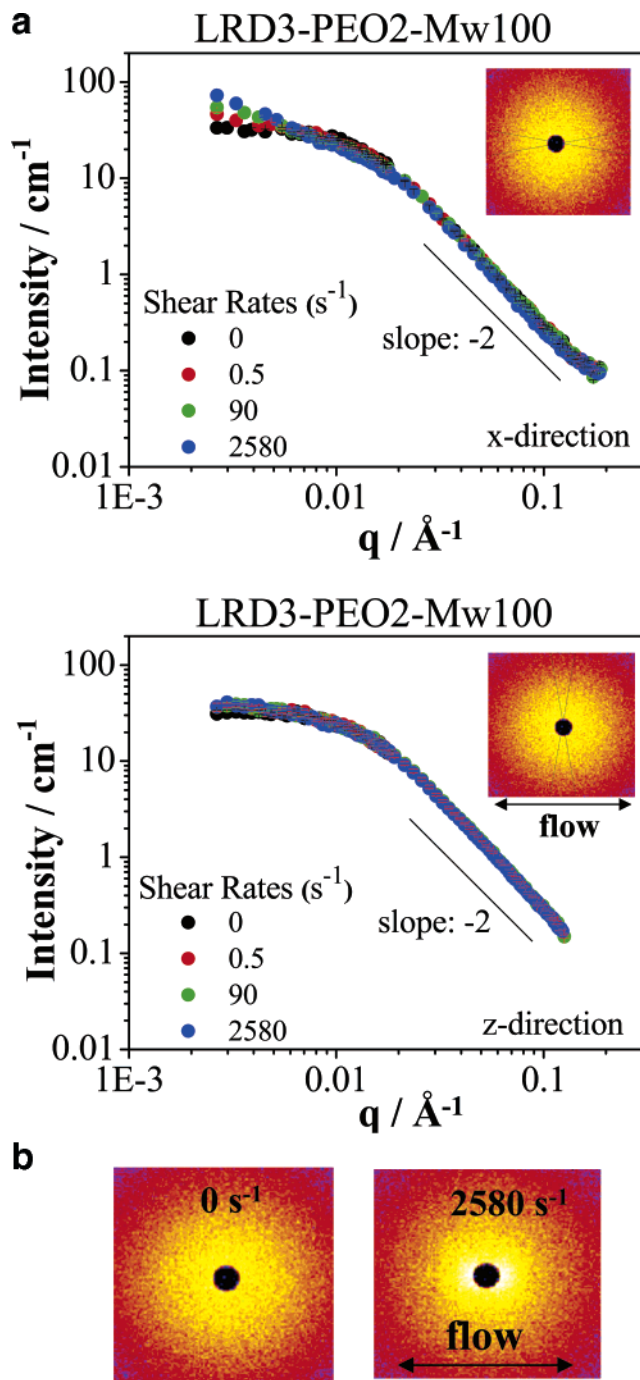
Figure 4. (a) I vs q SANS data for a LRD3-PEO2-M_w 100 gel in the q range of ($q = 4\pi/\lambda \sin(\theta)/2$), 2.27×10^{-3} Å^{-1} < q < 0.24 Å^{-1} and at different shear rates, averaged parallel (x-direction) and perpendicular (z-direction) to the flow. (b) 2D SANS patters as obtained from the sample at rest (0 s^{-1}) and at the highest measured shear rate (2580 s^{-1}).

exponents m ($\eta = (d\gamma/dt)^m$) which vary from $m = 0.6$ at high molecular weight to $m = 0.9$ at low M_w (Figure 3). The high shear rate data are limited due to normal forces that push the sample out of the shear cell, and variations from linearity are observed at the highest shear rates. The M_w dependence of the viscosity decreases significantly with decreasing shear rates, hinting at an identical viscosity at the low shear rates. This result is consistent with our hypothesis of long chains bridging clay platelets in a dynamic absorption–desorption equilibrium with a finite time constant. At low shear rates the mechanical coupling between clay platelets and long polymer chains has only marginal consequences on the flow properties. As the shear rate
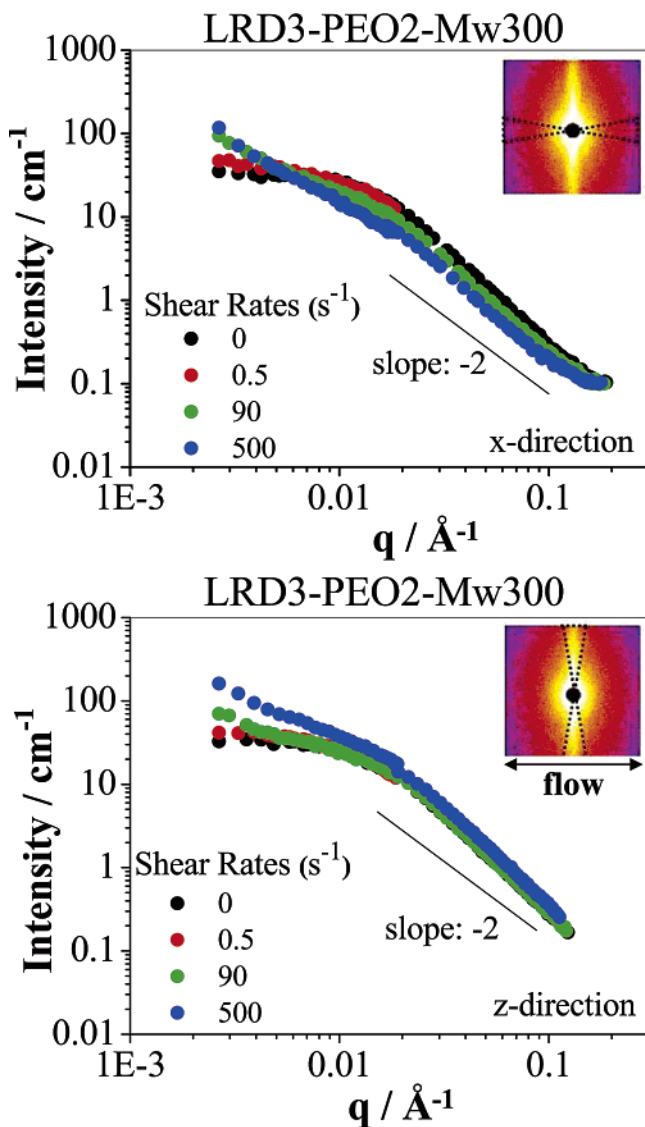
Figure 5. *I* vs *q* data for LRD3-PEO2-M_w 300 gel at rest (0 s^{-1}) and at a different shear rates average parallel and perpendicular to the flow direction. Insert: 2D SANS patters showing the sectors used for averaging *I*(*q*). A relative error is smaller than the symbols.

Figure 6. *I* vs *q* data for LRD3-PEO2-M_w 600 gel at rest (0 s^{-1}) and at a different shear rates average parallel and perpendicular to the flow direction. Insert: 2D SANS patters showing the sectors used for averaging *I*(*q*). A relative error is smaller than the symbols.

increases, any interactions become increasingly important and are reflected first in the steady-state viscosity which increases for a given shear rate in the series LRD3-PEO2-M_w 100, 300, 600, 1000 and then on the microstructural orientation as discussed below.

Figures 4, 5, and 6 show SANS data from the LRD3-PEO2-M_w 100, 300, and 600 gels, respectively, taken at rest and at different shear rates. No significant SANS anisotropy was detected for any of the data at rest. As the flow field is applied, a clear anisotropy develops for the higher molecular weights. All isotropic and anisotropic patterns were averaged in 10° sectors parallel (*x*-direction) and perpendicular (*z*-direction) to the flow to give *I* vs *q* in each direction. At rest the data exhibit a strong rollover expected of finite sized objects, and an apparent R_g can be calculated from a Guinier fit to be ≈10 nm, consistent with the $R_g = \sqrt{(R^2/2+H^2/12)}$ of 10.6 nm for 30 nm diameter disks of thickness $H = 1$ nm. The slope at high *q* of slightly more than the −2 expected for disklike structures[7,27,28] is not surprising given that the excess polymer also must contribute some to the scattering in this regime. Attempts to fit the full curves to a simple core + shell model similar to the one used by Nelson et al.[7] for dilute systems of PEO/Laponite fail for
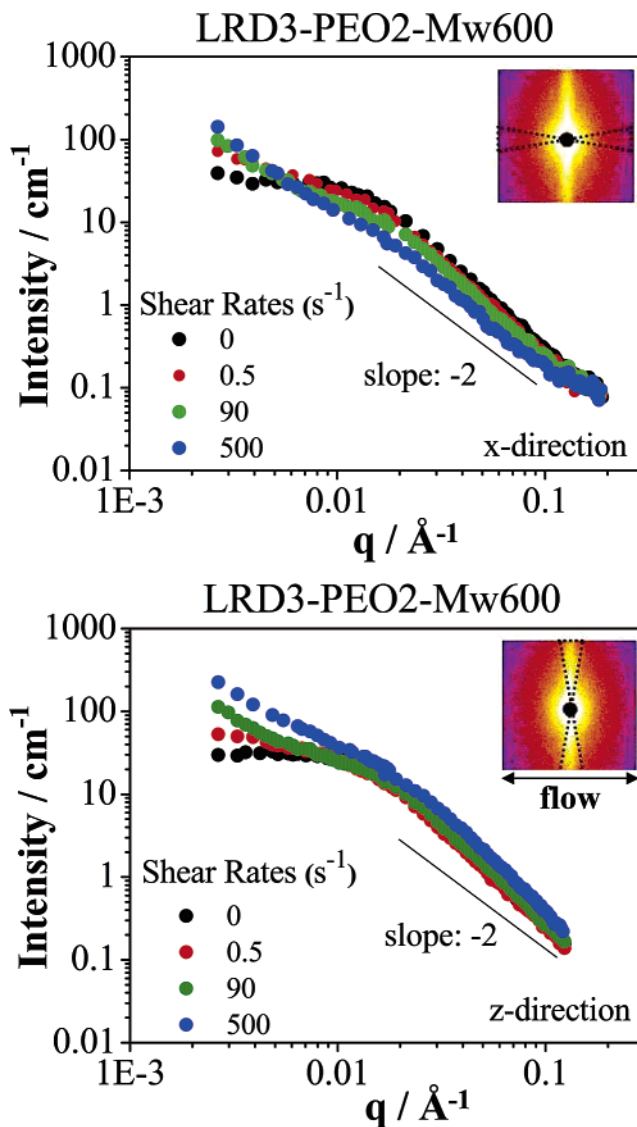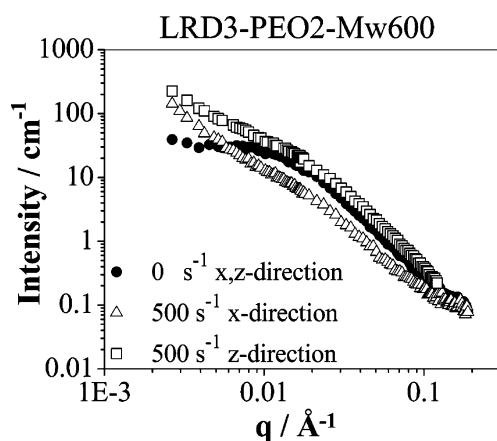

Figure 7. *I* vs *q* data for LRD3-PEO2-M_w 600 gel at rest (0 s^{-1}) and at a shear rate of 500 s^{-1}, averaged parallel (*x*-direction) and perpendicular (*z*-direction) to the flow.

all samples. While the presence of excess polymer would contribute to this problem, it is likely that in fact there may be some interaction (structure factor) effects also at play as was
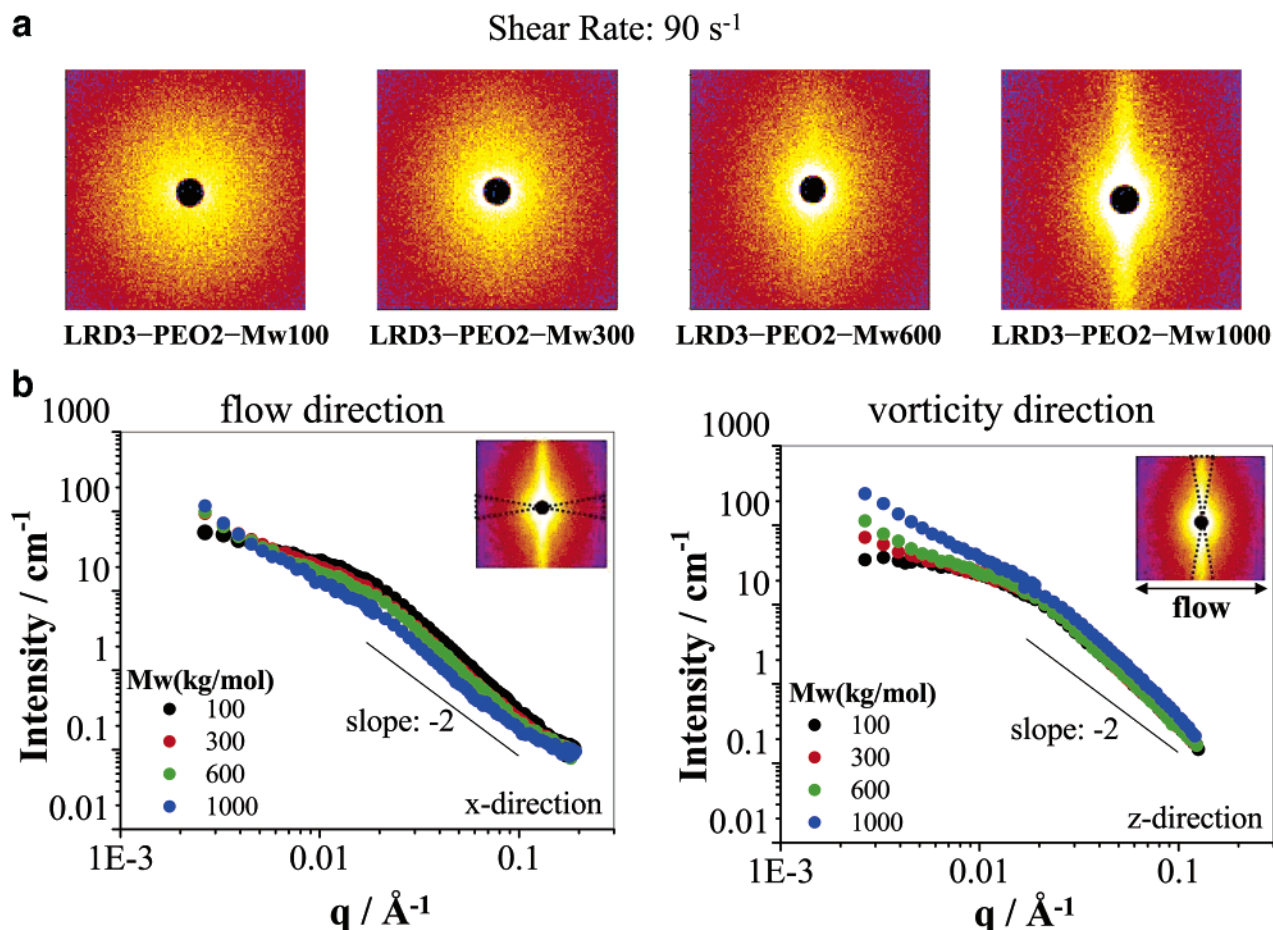
Figure 8. (a) 2D SANS profiles of samples at a shear rate of 90 s^{-1}. Anisotropic SANS patterns observed at the samples with $M_w = 300$, 600, and 1000. (b) Averaged intensity vs q for the samples with different molecular weight, at a shear rate of 90 s^{-1}. Left: intensity average parallel to the flow (x-direction). Right: intensity average perpendicular to the flow (z-direction). Inserts: 2D SANS anisotropic scattering patterns showing the sectors used for averaging the intensity.

found for systems of pure Laponite and that the rollover is not in fact due entirely to an R_g effect.

For the LRD3-PEO2-M_w 100 sample (Figure 4) the intensity in the z-direction (perpendicular to the flow) is more or less the same for all shear rates, while a slight upturn, at low q only, is observed at the higher shears in the x-direction (parallel to the flow). This contrasts, for example, with the higher molecular weights such as LRD3-PEO2-M_w 300 and 600 (Figures 5 and 6) where anisotropy is evident over the entire q regime at the higher shear rates, and the intensity curves parallel and perpendicular to the flow split above and below the data at rest (Figure 7). The curves parallel to the flow decrease relative to the at rest curve, indicating they are probing more of the longer dimension, and the curves perpendicular to the flow, increasing in intensity, are probing more of the shorter dimension. Thus, the platelets seem to be orienting with their normal parallel to the vorticity axis as discovered previously.[8] Figure 8 shows the molecular weight dependence of the anisotropy for a fixed shear rate of 90 s^{-1}. All but the lowest molecular weight exhibit anisotropy which increases as a function of increasing molecular weight.

Closer inspection of Figure 7 shows that both curves (parallel and perpendicular) increase above the "at rest curve" at the lowest q. This indicates that besides the nanoscale alignment of the platelets, there is a shear-induced larger-scale structure forming which is also anisotropic and aligning in the flow. It is interesting to note that while the LRD3-PEO2-M_w 100 sample shows no evidence of orientation of the platelets, it nonetheless

forms the oriented shear-induced structure. Our previous work on LRD3-PEO2-M_w 1000 showed[17] the existence of a very large scale spongelike structure, but its signature is well outside of the q range used here and thus not visible. However, these shear-induced structures are consistent with previous studies on similar systems which concluded that transient micron scale heterogeneities[25,26] develop during shear disappearing upon cessation of shear. The relaxation behavior after cessation of shear of these gels is currently not well understood. While SANS studies on representative LRD3-PEO2-M_w 1000 solutions observed very fast relaxation of anisotropy, stress-relaxation measurements show that full relaxation occurs at very long times.[29] This implies a fast orientational relaxation on the nanoscale but a much slower full stress relaxation mode in the material.

Figure 9 summarizes our SANS results by plotting the anisotropy, $|(I_z - I_v)/(I_z + I_v)|$, as a function of shear rate for each of the gels in the series (LRD3-PEO2-M_w 100, 300, 600, 1000). I_v and I_z correspond to the SANS intensity at $q = 0.01$ Å^{-1} from 0° (parallel to the flow) and 90° (perpendicular to the flow), respectively, and thus only measures the platelet alignment and not the larger scale structure. The LRD3-PEO2-M_w 1000 sample starts aligning below 1 s^{-1} while the LRD3-PEO2-M_w 300 and LRD3-PEO2-M_w 600 samples start aligning just above a shear rate of 30 and 10 s^{-1}, respectively. Given this trend, the fact that no anisotropy appears for the LRD3-PEO2-M_w 100 gel up to 2580 s^{-1} (at this q value) and the fact that the trends in the dynamic rheology of G' and G'' occurs between the 100 and 300 kg/mol samples, it is likely that there
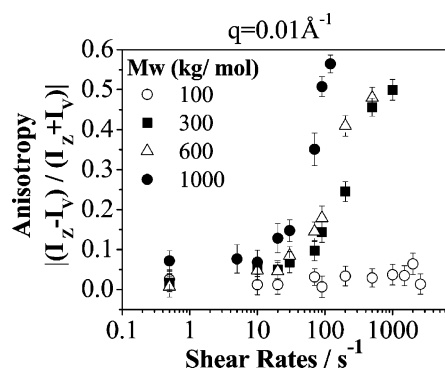
Figure 9. Anisotropy $(I_z - I_v)/(I_z + I_v)$ as a function of shear rate for the samples with different PEO M_w. I_v and I_z correspond to the SANS intensity at $q = 0.01$ Å^{-1} from 0° (parallel to the flow) and 90° (perpendicular to the flow), respectively.

is a critical M_w threshold somewhere between those two molecular weights. It is interesting that even though the LRD3-PEO2-M_w 100 gel shows no orientation of the nanoparticles, it exhibits stronger shear thinning behavior than the other samples. In fact, there is an inverse relationship between ease of orientation and shear thinning. This is consistent with the idea that particle orientation is driven by the interaction of a strongly connected network with the flow. The increasing strength of the connectedness that leads to increased orientation would also be expected to lower the rate of shear thinning.

Conclusion

From the data presented here, it is clear that the dynamics of these systems are strongly influenced by the ability of the polymer to bridge two or more clay platelets. Our results indicate that there exists a critical M_w between 100 and 300 kg/mol (for the system containing 3% LRD and 2% PEO), below which the system behaves rheologically very similarly to the pure clay systems and does not exhibit shear-induced nanoscopic orientational ordering. However, once the polymer is long enough to interconnect several clay platelets, platelet alignment is clearly visible at rather low deformations with an onset shear rate that increases with decreasing molecular weight. The interconnectedness is also reflected in the steady-state viscosities which exhibit a decreasing amount of shear thinning as the interconnectedness increases. The existence of a shear-induced structure both above and below the bridging threshold suggests that this structure is due to other mechanisms than the dynamic cross-linking postulated for most of the phenomena discussed here.

References and Notes

(1) Lovinger, A. J. *J. Macromol. Sci., Part C* **2005**, *45*, 195−199.
(2) Krishnamoorti, R.; Vaia, R. A. *Polymer Nanocomposites−Synthesis, Characterization and Modeling*; American Chemical Society: Washington, DC, 2001; Vol. 804.
(3) Chapman, R.; Mulvaney, P. *Chem. Phys. Lett.* **2001**, *349*, 358−362.
(4) Wilson, O.; Wilson, G. J.; Mulvaney, P. *Adv. Mater.* **2002**, *14*, 1000.
(5) Yoon, P. J.; Fornes, T. D.; Paul, D. R. *Polymer* **2002**, *43*, 6727−6741.
(6) Swenson, J.; Smalley, M. V.; Hatharasinghe, H. L. M.; Fragneto, G. *Langmuir* **2001**, *17*, 3813−3818.
(7) Nelson, A.; Cosgrove, T. *Langmuir* **2004**, *20*, 2298−2304.
(8) Schmidt, G.; Nakatani, A. I.; Butler, P. D.; Han, C. C. *Macromolecules* **2002**, *35*, 4725−4732.
(9) Ho, D. L.; Glinka, C. J. *Chem. Mater.* **2003**, *15*, 1309−1312.
(10) Mongondry, P.; Nicolai, T.; Tassin, J. F. *J. Colloid Interface Sci.* **2004**, *275*, 191−196.
(11) Schmidt, G.; Nakatani, A. I.; Butler, P. D.; Karim, A.; Han, C. C. *Macromolecules* **2000**, *33*, 7219−7222.
(12) Schmidt, G.; Nakatani, A. I.; Han, C. C. *Rheol. Acta* **2002**, *41*, 45−54.
(13) Zebrowski, J.; Prasad, V.; Zhang, W.; Walker, L. M.; Weitz, D. A. *Colloids Surf., A* **2003**, *213*, 189−197.
(14) Lal, J.; Auvray, L. *Mol. Cryst. Liq. Cryst.* **2001**, *356*, 503−515.
(15) Lal, J.; Auvray, L. *J. Appl. Crystallogr.* **2000**, *33*, 673−676.
(16) Smalley, M. V.; Hatharasinghe, H. L. M.; Osborne, I.; Swenson, J.; King, S. M. *Langmuir* **2001**, *17*, 3800−3812.
(17) Loizou, E.; Butler, P. D.; Porcar, L.; Talmon, Y.; Kesselman, E.; Schmidt, G. *Macromolecules* **2005**, *38*, 2047−2049.
(18) Certain equipment and instruments or materials are identified in this paper in order to adequately specify the experimental details. Such identification does not imply recommendation by the National Institute of Standards and Technology nor does it imply the materials are the best available for the purpose.
(19) Glinka, C. J.; Barker, J. G.; Hammouda, B.; Krueger, S.; Moyer, J. J.; Orts, W. J. *J. Appl. Crystallogr.* **1998**, *31*, 430−445.
(20) Straty, G. C.; Hanley, H. J. M.; Glinka, C. J. *J. Stat. Phys.* **1991**, *62*, 1015−1023.
(21) Ramsay, J. D. F.; Lindner, P. *J. Chem. Soc., Faraday Trans.* **1993**, *89*, 4207−4214.
(22) Saunders, J. M.; Goodwin, J. W.; Richardson, R. M.; Vincent, B. *J. Phys. Chem. B* **1999**, *103*, 9211−9218.
(23) Callaghan, I. C.; Ottewill, R. H. *Faraday Discuss.* **1974**, *57*, 110.
(24) Obtained by DLS from dilute solutions.
(25) Lin-Gibson, S.; Kim, H.; Schmidt, G.; Han, C. C.; Hobbie, E. K. *J. Colloid Interface Sci.* **2004**, *274*, 515−525.
(26) Lin-Gibson, S.; Schmidt, G.; Kim, H.; Han, C. C.; Hobbie, E. K. *J. Chem. Phys.* **2003**, *119*, 8080−8083.
(27) Pignon, F.; Magnin, A.; Piau, J. M.; Cabane, B.; Lindner, P.; Diat, O. *Phys. Rev. E* **1997**, *56*, 3281−3289.
(28) Kroon, M.; Vos, W. L.; Wegdam, G. H. *Phys. Rev. E* **1998**, *57*, 1962−1970.
(29) Malwitz, M. M.; Butler, P. D.; Porcar, L.; Angelette, D. P.; Schmidt, G. *J. Polym. Sci., Part B: Polym. Phys.* **2004**, *42*, 3102−3112.